Catalysis Surveys from Asia (2022) 26:346–357
https://doi.org/10.1007/s10563-022-09374-8

ORIGINAL ARTICLE

In-situ One-Pot Synthesis of Ti/Cu-SSZ-13 Catalysts with Highly Efficient NH_3-SCR Catalytic Performance as Well as Superior H_2O/SO_2 Tolerability

Jie Wan[1,2] · Jiawei Chen[2] · Yijun Shi[2] · Yiyan Wang[2] · Yanjun Liu[1] · Jin Zhang[1] · Gongde Wu[1] · Renxian Zhou[2]

Received: 28 May 2022 / Accepted: 22 September 2022 / Published online: 29 September 2022

Abstract
Series of Ti/Cu-SSZ-13 zeolite catalysts with variable Ti content were prepared via convenient *in-situ* one-pot synthesizing strategy. Systematic evaluations of the NH_3-SCR catalytic performance over the obtained catalysts were conducted. Results show that Ti/Cu-SSZ-13 with appropriate Ti content (in the current work $Ti_{0.81}/Cu_{2.15}$-SSZ-13) could serve as capable candidate for NH_3-SCR application, as it exhibits highly efficient catalytic activity with expanded operation temperature window width from 140 to 540 °C, nearly 100% N_2 selectivity, as well as superior tolerability against water vapor and SO_2. Further structural/physicochemical characterizations demonstrate that the obtained Ti/Cu-SSZ-13 catalysts possess well-crystallized characteristic chabazite (CHA) structure. Isolated Cu^{2+} and monomeric Ti^{4+} are recognized as the primary active species, as the former mainly contributes to SCR reaction at low temperatures, while the latter are conducive for improving the high temperature SCR activity. Ti over doping would result in partial destruction of the zeolite structure, occupation of Cu^{2+} cation sites and formation of surface aggregated TiO_x, thus leading to unsatisfactory NH_3-SCR performances. Moreover, formation of agglomerated CuO_x species during hydrothermal ageing and blockage of surface active sites by sulfate species formed during SO_2 pretreatment are considered responsible for activity deterioration in the tolerability tests.

Keywords Cu-SSZ-13 · Titanium doping · NH_3-SCR · Active species · One-pot synthesis · SO_2-poisoning

1 Introduction

The rapid development of modern transportation has brought great convivence to modern society, but the vehicle exhaust pollution has been come one of the most pressing threats to both environmental sustainability and human health simultaneously. Diesel engine vehicles with lean combustions technology have attracted more and more attentions in automobile industry, owning to their higher thermal efficiency as well as low hazardous exhaust emission [1, 2]. Yet, nitrogen oxides (NO_x) emitted from diesel vehicles are recognized as main culprit for acid rain, photochemical smog, ozone layer depletion, as well as human respiratory and cardiovascular diseases [3, 4]. Among various techniques developed for eliminating NO_x emission in diesel engine exhaust, selective catalytic reduction of NO_x using NH_3 as reductant (NH_3-SCR) has been widely employed as the most practical and effective approach [5, 6]. Highly efficient catalysts are the critical materials for NH_3-SCR technology. V_2O_5-WO_3-TiO_2 complex oxides (VWTi) have become the most widely employed commercial catalysts in SCR systems since early 1970s [7, 8]. Nevertheless, with more progressively strict emission regulations and fuel efficiency standards, serious challenges are raised against VWTi systems such as insufficient performance under lean combustion condition, limited operation temperature window width, unsatisfactory thermal stability, weak tolerability against SO_2 let along the toxic effect of V^{5+} containing substance [9–11], therefore pushing forward the growing needs for investigating novel catalysts for SCR application.

Over the past few decades, Cu-based zeolites have aroused considerable research attention. For instance, Cu-ZSM-5, Cu-beta, Cu-USY, and Cu-SAPO-34 etc. [12–14] have all been proposed advantageous for NH_3-SCR. Among

✉ Renxian Zhou
zhourenxian@zju.edu.cn

1 Energy Research Institute, Nanjing Institute of Technology, Nanjing 211167, People's Republic of China

2 Institute of Catalysis, Zhejiang University, Hangzhou 310028, People's Republic of China

various zeolites explored, Cu-SSZ-13 zeolites with characteristic chabazite (CHA) structure are currently the most state-of-the-art materials [15–17]. Gao et al. [18] reported that Cu-SSZ-13 presented superior NH_3-SCR activity, low selectivity towards N_2O and relative higher hydrothermal stability comparing to either Cu-beta or Cu-ZSM-5. Kwak et al. [19] reported Cu-SSZ-13 could maintain remarkable catalytic activity between 300 and 400 °C even after rigorous hydrothermal ageing. On the other hand, maintaining SCR reactivity at higher temperature range is of equal importance for developing novel SCR catalysts, since the exhaust gas could be extremely hot especially during vehicle rapid acceleration. Unfortunately, Cu/SSZ-13 catalysts display insufficient SCR reactivity at temperatures above 450 °C, which severely hinders its practical applications [20]. Various researchers [21–23] have proposed that one possible solution is doping transitional metals into Cu-SSZ-13. For example, Cu/Fe-SSZ-13 catalyst [24–26] is reported to exhibited enhanced activity with relatively broadened operation temperature window width, but its high-temperature selectivity and tolerability against H_2O/SO_2 still needs further alleviation [27–29]. Ti as transitional metal with weak acidity, presents similar chemical properties to Cu and Fe, and has good resistance to sulfur poisoning. Ti^{4+} ions can also better coordinate into Si-Al zeolites framework and sever as active centers without changing the original zeolite topology. Therefore, constructing Ti/Cu-SSZ-13 system with proper composition control might be potentially promising for optimizing NH_3-SCR reactivity at more broadened temperature range. Also, the possible connections between the catalytic performance and active species requires further exploration to provide theoretical support. Moreover, the traditional method for synthesizing of SSZ-13 zeolite requires the addition of high-price organic template agent (N,N,N-trimethyl-1-adamantammonium hydroxide, TMAdaOH) and multi-step ion-exchange procedures [30], making the preparation of bimetallic SSZ-13 catalysts very complicated, costly and unpractical for industrial application. Thus, developing simple one-pot strategy for synthesizing Ti/Cu-SSZ-13 catalyst is also very necessary.

In the present work, Ti/Cu-SSZ-13 zeolite catalysts with variable Ti loading content were prepared via *in-situ* one-pot synthesizing strategy. The prepared Ti/Cu-SSZ-13 catalysts were subjected to NH_3-SCR catalytic performances evaluation including activity tests as well as durability tests against H_2O/SO_2. Detailed characterizations such as X-ray diffraction (XRD), Hydrogen temperature-programmed reductions (H_2-TPR), X-ray photoelectron spectroscopies (XPS) and ultraviolet visible spectroscopies (UV–Vis) were also performed. The scope of this work is (i) to propose Ti/Cu-SSZ-13 zeolite catalysts with excellent NH_3-SCR activity and durability using effective one-pot synthesizing strategy along with proper composition tuning; and (ii) to gain possible new insights into the effect of Ti doping on the structure–activity correlations of NH_3-SCR reaction over Ti/Cu-SSZ-13 zeolites.

2 Experimental Section

2.1 Catalysts Preparation

2.1.1 Syntheses of Ti/Cu-SSZ-13 Zeolites

Ti/Cu-SSZ-13 zeolites with variable Ti loading content were synthesized via *in-situ* one-pot strategy according to following steps: (i) certain quantity of $CuSO_4$·was dissolved in deionized water and kept stirring for 0.5 h; (ii) then 1.2 g Tetraethylenepentamine (TEPA) was injected and stirred for another 1 h; (iii) $C_{10}H_{14}O_5Ti$ was chosen as Titanium source and was added into the solution along with certain amount of NaOH and NaAlO sequentially; (iv) 3.6 mL colloidal silica was dripped dropwise under 3 h continuous stirring; (v) the mixed solution was transferred to a 100 mL Teflon lined stainless steel autoclave and hold on at 140 °C for 96 h hydrothermal reaction; (vi) the hydrothermal product was dried at 100 °C overnight followed by 12 h acid-leaching with dilute nitric acid at 80 °C; (vii) the obtained precursor was finally calcined at 550 °C in a muffle furnace for 4 h to acquire the designed catalyst.

The different Ti loading content was controlled by varying $C_{10}H_{14}O_5Ti$ quantity (i.e., $x = 0$, 0.05, 0.1, 0.15, 0.2, 0.25) and the actual Ti/Cu content of the prepared Ti/Cu-SSZ-13 zeolites was validated using ICP-AES analyses. The obtained catalysts were denoted according to the corresponding ICP results as $Ti_{0.40}/Cu_{2.53}$-SSZ-13, $Ti_{0.52}/Cu_{2.38}$-SSZ-13, $Ti_{0.81}/Cu_{2.15}$-SSZ-13, $Ti_{1.08}/Cu_{1.68}$-SSZ-13 and $Ti_{1.34}/Cu_{1.47}$-SSZ-13, respectively (subscript numbers representing different weight percentage).

2.1.2 Hydrothermal Ageing and SO_2 Pretreatment

The obtained Ti/Cu-SSZ-13 sample with the most outstanding SCR activity was subjected to hydrothermal ageing at 750 °C for 24 h using air flow with 10 vol. % steam. The hydrothermal aged catalysts were designated using suffix "-aged".

Similarly, the optimized Ti/Cu-SSZ-13 sample were also put through SO_2 pretreatment at 350 °C for 16 h using 100 ppm SO_2 with Ar as balancing gas flow. Catalysts after SO_2 pretreatment were designated using as suffix "-SO_2".

All the mentioned catalysts were tableted, grinded, and sieved to approximately 40 to 60 mesh before conducting further tests.

2.2 NH_3-SCR Catalytic Performance Tests

NH_3-SCR catalytic performance tests were performed using self-construct fixed bed reactor. The reaction atmosphere contains 5 vol. % O_2, 500 ppm NO_x (490 ppm NO + 10 ppm NO_2), 500 ppm NH_3 and Ar are used as balancing gas. The inlet reaction gas flow was set at an hourly space velocity (GHSV) of 50,000 h^{-1}. Actual composition of both inlet and outlet gas was analyzed online quantitatively using an FTIR spectrometer (Bruker EQUINOX 55, Bruker Corporation, United States) attached with a multi-pass gas cell (1.33 L cell volume and 10.0 m light path length). NO_x conversions and N_2 selectivity were determined based on the following Eqs. (1) and (2):

$$C_{NO_x} = \frac{NO_{x\text{ - inlet}} - NO_{x\text{ - outlet}}}{NO_{x\text{ - inlet}}} \times 100\% \quad (1)$$

$$S_{N_2} = \frac{2N_{2\text{ - outlet}}}{NO_{x\text{ - intlet}} + NH_{3\text{ - inlet}} - NO_{x\text{ - outlet}} - NH_{3\text{ - outlet}}} \times 100\% \quad (2)$$

2.3 Catalysts Characterizations

X-ray diffraction analyses (XRD) was performed on an X-ray diffractometer (Shimazu XRD 7000, SHIMADZU Corporation, Japan) equipped with monochromated Cu Kα radiation. The diffractograms were recorded from 5° to 70° (2θ) at 0.02° step size. H_2 temperature-programmed reductions (H_2-TPR) were carried out on an automatic chemisorption apparatus (ChemBET3000, Quantachrome Instruments, USA). 100 mg sample was first pretreated at 400 °C using 40 mL min^{-1} Ar flow for 30 min. Upon cooling down to 50 °C, 5 vol. % H_2/Ar was introduced into the reactor with 40 mL min^{-1} flow rate till baseline stabilization. The reactor temperature was elevated to 950 °C at 10 °C min^{-1} ramping rate and H_2-TPR profiles were collected synchronously by measuring thermal conductivity detector (TCD) signals. X-ray photoelectron spectroscopies (XPS) were performed on a Thermo ESCALAB 250Xi apparatus (Themo Fisher Scientific Corporation, USA) employed with monochromatic Al *K*α source. C 1 s peak at 284.8 eV were used as internal label to calculate binding energies of each element tested. Ultraviolet visible spectroscopies (UV–Vis) were performed on a UV/Vis spectrometer (UV 2450, SHIMADZU Corporation, Japan). Sepctra were recorded at room temperature with wavelength ranging from 200 to 800 nm and $BaSO_4$ was referenced as background.

3 Results and Discussion

3.1 NH_3-SCR Catalytic Performances

Figure 1a presents the NO_x conversion plots of the synthesized Ti/Cu-SSZ-13 catalysts. The operation temperature window width (corresponding temperature ranges wherein NO_x conversion stays above 90%) follows the sequence as: $Ti_{0.81}/Cu_{2.15}$-SSZ-13 (140–540 °C) > $Ti_{1.08}/Cu_{1.68}$-SSZ-13 (140–530 °C) > $Ti_{0.52}/Cu_{2.38}$-SSZ-13 (140–520 °C) > $Ti_{1.34}/Cu_{1.47}$-SSZ-13 (145–505 °C) > $Ti_{0.40}/Cu_{2.53}$-SSZ-13 (145–495 °C) > $Cu_{3.25}$-SSZ-13 (145–490 °C). In comparison with $Cu_{3.25}$-SSZ-13 catalysts, although the low temperature activity has no obvious change (T_{90} value are quite similar at temperature below 200 °C), the high temperature activity of Ti/Cu-SSZ-13 is clearly improved first and then starts to decrease with increasing Ti content, making the operation temperature window width broadened first and then narrowed. It is worth noticing

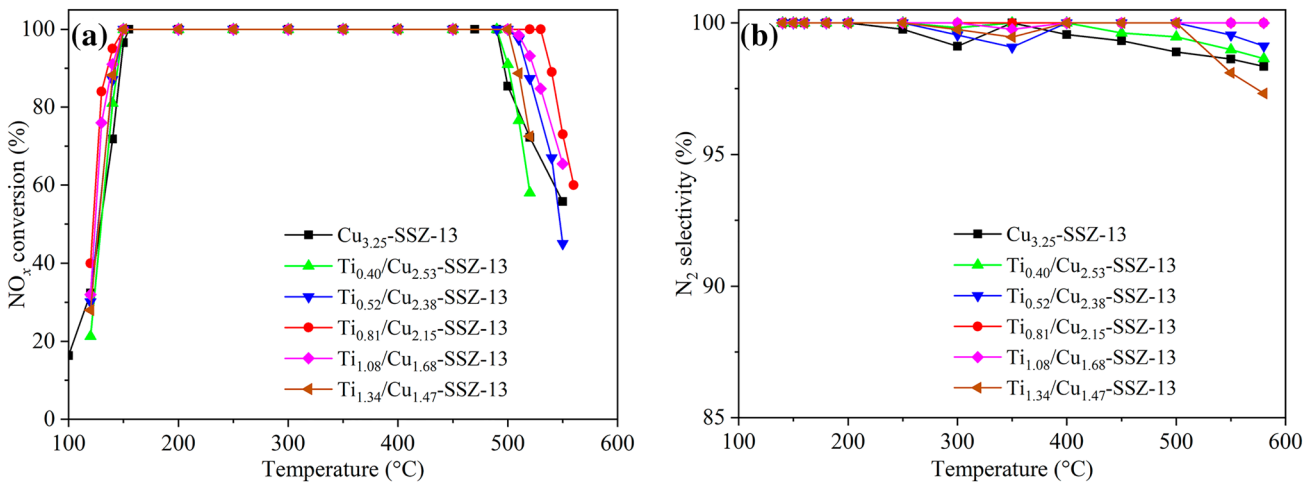

Fig. 1 NH_3-SCR catalytic performance results of the prepared Ti/Cu-SSZ-13 catalysts. **a** NO_x conversion, **b** N_2 selectivity

that the $Ti_{0.81}/Cu_{2.15}$-SSZ-13 catalyst (i.e., with 0.81 wt.% Ti content) displays the most broadened operation temperature window width from 140 to 540 °C, which suggests that doping appropriate amount of Ti into Cu-SSZ-13 can significantly promote the high-temperature activity for NH_3-SCR reaction. Figure 1b shows the N_2 selectivity over the prepared Ti/Cu-SSZ-13 catalysts. As can be seen, all the Ti/Cu-SSZ-13 catalysts possess over 95% N_2 selectivity, especially for $Ti_{0.81}/Cu_{2.15}$-SSZ-13 catalyst which shows nearly 100% N_2 selectivity during the whole testing temperature range. These results suggest that Ti/Cu-SSZ-13 catalyst with proper Ti doping content (in this work 0.81 wt.%) presents catalytic advantages comparing to single Cu-SSZ-13 and could be capable for efficent NO_x elimination.

3.2 Catalysts Tolerability Against H_2O/SO_2

Tolerability of the zeolite-based catalysts against H_2O/SO_2 is another crucial aspect for evaluating the practicality regarding the purification of diesel engine exhaust. On one hand, these catalysts generally operate long-time in high temperature exhaust gas containing large proportion of water vapor, which are prone to problems such as dealumination, structure collapse or active species sintering, causing activity deterioration. On the other hand, trace amount of sulfur-containing components in the exhaust gas can easily cause catalysts poisoning, which has long been critical issues for elongating catalysts lifetime. Based on the activity results above, to further evaluating the tolerability against H_2O/SO_2, we herein choose $Ti_{0.81}/Cu_{2.15}$-SSZ-13 catalyst as the most outnstanding candidate and subsquentially underwent hydrothermal ageing as well as SO_2 pretreatment before conducting NH_3-SCR tests.

3.2.1 Hydrothermal Ageing

Figure 2 shows the NH_3-SCR catalytic performance of $Ti_{0.81}/Cu_{2.15}$-SSZ-13 and $Cu_{3.25}$-SSZ-13 catalysts beofore and after hydrothermal ageing. For $Cu_{3.25}$-SSZ-13, drastically diminution of the operation temperature window width occurs after hydrothermal ageing (fresh: 145–490 °C and aged: 160–450 °C). While for $Ti_{0.81}/Cu_{2.15}$-SSZ-13 catalyst, the operation temperature window can be preserved from 175 to 490 °C after 24 h hydrothermal ageing. Although the the operation temperature window of $Ti_{0.81}/Cu_{2.15}$-SSZ-13-aged was deteriorated about 70 °C compared to the fresh catalyst, it still shows clear advantages over single $Cu_{3.25}$-SSZ-13. Meanwhile, Fig. 2b also shows that N_2 selecvitiy of $Ti_{0.81}/Cu_{2.15}$-SSZ-13 at high temperature range (> 450 °C) is slightly dropped after hydrothermal ageing, but it still remains quite advantagous comparing to $Cu_{3.25}$-SSZ-13-aged. These results validate that doping an appropriate amount of Ti into Cu-SSZ-13 catalyst can also benefiting its tolerability against water vapor as well as maintaining excellent N_2 selecvitiy.

3.2.2 SO_2 Pretreatment

The tolerability against sulfur poisoning of $Ti_{0.81}/Cu_{2.15}$-SSZ-13 catalyst was evaluated by SO_2 pretreatment tests. As shown in Fig. 3a, the operation temperature window of $Cu_{3.25}$-SSZ-13 ranges from 165 to 470 °C after 16 h SO_2 pretreatment at 350 °C. While for $Ti_{0.81}/Cu_{2.15}$-SSZ-13 catalyst, the operation temperature window stays from 180 to 520 °C after SO_2 pretreatment. The operation temperature window

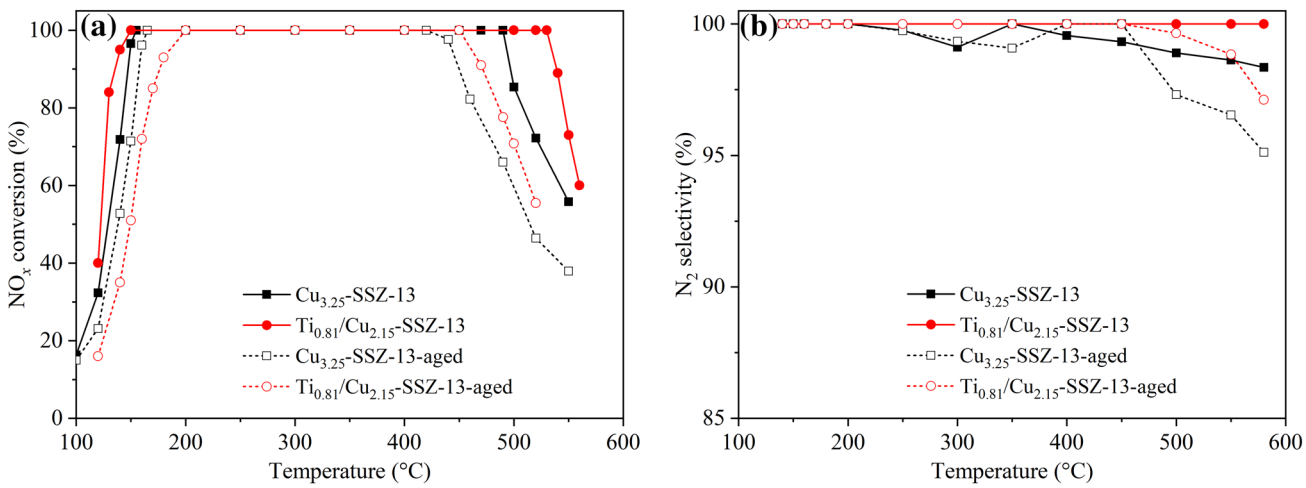

Fig. 2 NH_3-SCR results of $Ti_{0.81}/Cu_{2.15}$-SSZ-13 and $Cu_{3.25}$-SSZ-13 catalysts before/after hydrothermal ageing. **a** NO_x conversion, **b** N_2 selectivity

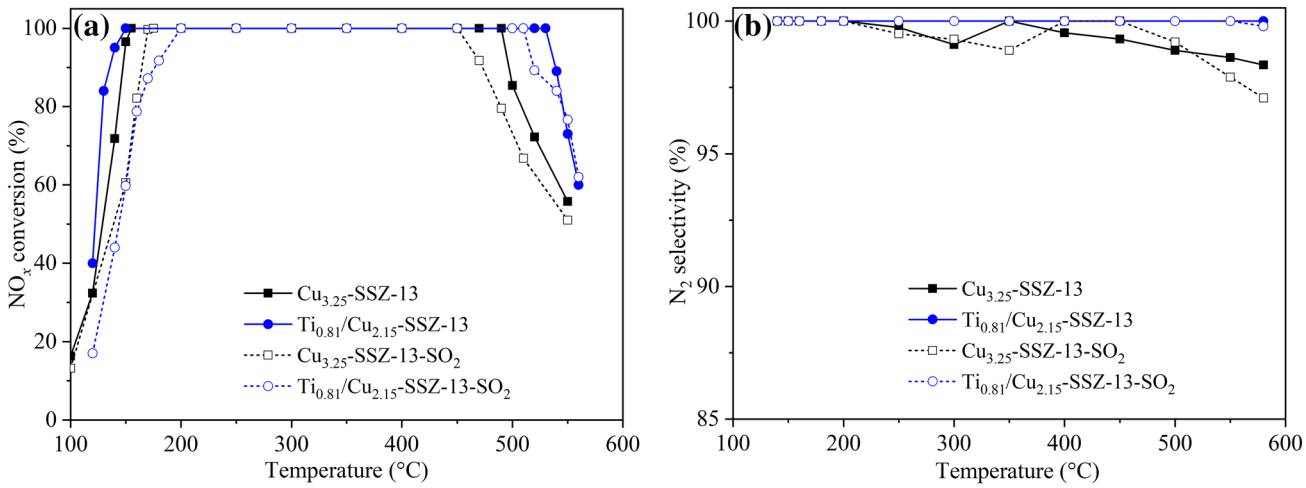

Fig.3 NH_3-SCR results of $Ti_{0.81}/Cu_{2.15}$-SSZ-13 and $Cu_{3.25}$-SSZ-13 catalysts before/after SO_2 pretreatment. **a** NO_x conversion, **b** N_2 selectivity

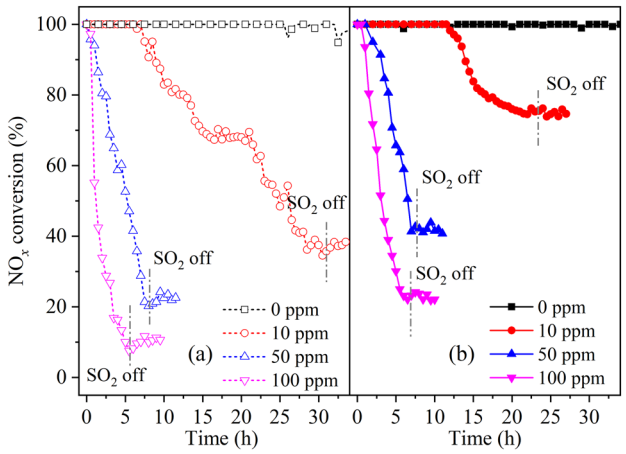

Fig. 4 Results of SO_2 "on/off" tests with different injection concentration during NH_3-SCR reaction. **a** $Cu_{3.25}$-SSZ-13, **b** $Ti_{0.81}/Cu_{2.15}$-SSZ-13

deterioration induced by SO_2 pretreatment is relatively more moderate than that of hydrothermal ageing. Similarly, despite its slightly hindered low temperature activity after SO_2 pretreatment, $Ti_{0.81}/Cu_{2.15}$-SSZ-13-SO_2 still maintains much better NO*x* eliminating capability at high temperatures than $Cu_{3.25}$-SSZ-13-SO_2 along with more broadened operation temperature window, as notably its T_{90} value in the high temperature range was only deteriorated by 20 °C. Besides, high N_2 selectivity (~ 100%) over $Ti_{0.81}/Cu_{2.15}$-SSZ-13-SO_2 can still be observed after SO_2 pretreatment (Fig. 3b). These resutls demonstrate that the superior toleratbility againsts sulfur-poisoning can be achieved by doping appropriate amount of Ti.

In order to better simulate actual operating condition for exhaust purification of diesel engines, SO_2 poisoning tolerability of $Ti_{0.81}/Cu_{2.15}$-SSZ-13 catalyst was further evaluated by applying SO_2 "on/off" testing method during SCR reaction. As shown in Fig. 4, for both $Ti_{0.81}/Cu_{2.15}$-SSZ-13 and $Cu_{3.25}$-SSZ-13 samples, the NO_x conversions remain stable around 100% before injecting SO_2 into the SCR reaction inlet gas. Once SO_2 is injected, immediate drop of NO_x conversion over both catalysts can be observed. Higher concentration of injected SO_2 could result in more drastically deteriorated SCR reactivity. For $Cu_{3.25}$-SSZ-13, only about 35% NO_x conversion gets to be retained after 30 h reaction with 10 ppm SO_2 injection. Increasing SO_2 concentration above 50 ppm causes more severe damage as it takes less than 5 h for the NO_x conversion to drop below 50%. When SO_2 concentration increased to 100 ppm, the SCR activity was almost completely deteriorated after 5 h reaction. These results indicate poor tolerability against sulfur poisoning of single Cu-SSZ-13 catalyst. For $Ti_{0.81}/Cu_{2.15}$-SSZ-13 catalyst, NO_x conversion can hold on to nearly 100% for 12 h with 10 ppm SO_2 injection and can remain above 75% after 30 h. Increasing SO_2 concentration to 50 ppm, full conversion of NO_x (~ 100%) can still be retained for more than 5 h. Continuing to increase SO_2 concentration to 100 ppm, NO_x conversion can maintain about 20% after the initial 5 h reaction. Such significant differences further demonstrate the superiority of $Ti_{0.81}/Cu_{2.15}$-SSZ-13 in toleratbility againsts sulfur-poisoning. Besides, once SO_2 is remove away from the reaction inlet, NO_x conversion over neither $Ti_{0.81}/Cu_{2.15}$-SSZ-13 nor $Cu_{3.25}$-SSZ-13 was able to return to the original stage. These results imply that the SO_2 poisoning cannot be simply explained by the competitive adsorption between SCR reactant and SO_2, but rather attributed to active sites blockage by the formation sulfate species.

Based on all the above results, it is well demonstrated that doping Cu-SSZ-13 catalysts with appropriate amount of Ti can not only improve the NH_3-SCR activity, but also increase its tolerability against hydrothermal ageing and

SO_2 poisoning. $Ti_{0.81}/Cu_{2.15}$-SSZ-13 catalyst in this work presents widely broadened operation temperature window, excellent N_2 selectivity as long with superior H_2O/SO_2 tolerability, making it potentially capable candidates for NH_3-SCR application in diesel engine vehicles.

3.3 Crystalline Structure by XRD

The crystal phase structures of the Ti/Cu-SSZ-13 catalysts were characterized by XRD analyses (Fig. 5). Characteristics diffraction peaks locating at (2θ = 9.5°, 12.8°, 14.0°, 16.1°, 17.8°, 20.7°, 25.0° and 30.7° can be observed on all the samples, which can be assigned to typical chabazite (CHA) structure (JCPDS #34-0137) [20, 31]. The sharp and clear peak shapes along with relatively high intensity reflects the formation of good crystallinity and further demonstrates that the *in-situ* one-pot synthesis strategy in this work are quite successful. Neither of the diffraction peaks assigning to CuO_x (2θ = 35.6° and 38.8°) nor TiO_x (2θ = 36.8°, 37.6 °, and 39.1°) can be observed, which can be explained as the content are too low to be detected by XRD or the copper/titanium oxide species are well distributed in the zeolite matrix [32]. With increasing Ti content, the intensity of CHA characteristic peaks gradually decreased with broaden peak shape, indicating that higher Ti introduction can lead to relatively weakened zeolite crystallinity. Such crystallinity decrease could result from the incorporation of Ti ions into the zeolite framework. Due to the same coordinate numbers of Ti^{4+} and Si^{4+} ions, Ti^{4+} ions are most likely to substitute part of Si^{4+} ions in the zeolite framework to form a tetrahedral coordination structure [33]. The ionic radius of Ti^{4+} is larger than Si^{4+} ions, thus Ti^{4+} incorporation will expand the interplanar spacing and cause partial destruction of the zeolite structure. On the other hand, with increasing Ti content, some of the cation sites in the zeolite cages will also be occupied by Ti^{4+} ions, which could impair the capacity to accommodate Cu^{2+} species, therefore the number of Cu species entering the SSZ-13 cages will also decreased. Moreover, textural characterization results of $Cu_{3.25}$-SSZ-13 and $Ti_{0.81}/Cu_{2.15}$-SSZ-13 (see the supplymentary information) show that Ti introduction would lead to slightly decreased specific surface area along with and pore volume, which might be related to the blockage of microporous channels by part of the Ti species. SEM photos of $Cu_{3.25}$-SSZ-13 and $Ti_{0.81}/Cu_{2.15}$-SSZ-13 were also recorded to give direct observation of the catalysts' morphologies (Fig. S1 in the supplymentary information), and the results shown that both samples present similar morphologies consisting of cube-shaped crystals, which suggests that doping small amount of Ti into Cu-SSZ-13 zeolites does not change the zeolite morphology. Correlating the activity results of $Cu_{3.25}$-SSZ-13 and $Ti_{0.81}/Cu_{2.15}$-SSZ-13, it's reasonable to say that such textural/morphological properties change here in our work may not be the key factor determining SCR activity.

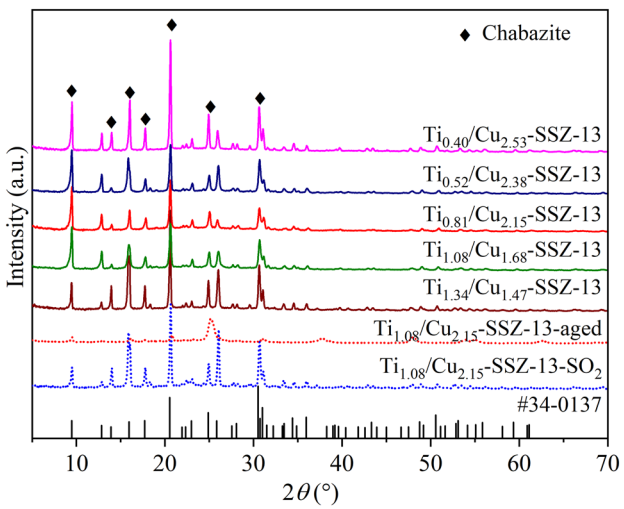

Fig. 5 XRD profiles of the prepared Ti/Cu-SSZ-13 catalysts

XRD profiles of $Ti_{0.81}/Cu_{2.15}$-SSZ-13 catalysts after hydrothermal ageing and SO_2 pretreatment are also presented in Fig. 5. For $Ti_{0.81}/Cu_{2.15}$-SSZ-13-aged, although obvious broadened peaks with decreased intensity can be seen, most of the featured CHA structure can be preserved in a certain degree, indicating that the zeolite structure is not completely destroyed during hydrothermal ageing but rather partial crystallinity damage and formation of amorphous phase. Such structure evolutions are likely to be one of the reasons explaining the inferior SCR activity upon hydrothermal ageing. For $Ti_{0.81}/Cu_{2.15}$-SSZ-13-SO_2, there is no significant changes in the diffraction profiles, suggesting that SO_2 pretreatment does not bring much impact to the crystalline structure of $Ti_{0.81}/Cu_{2.15}$-SSZ-13 catalyst, which is also an important reason explaining why its SCR performance does not deteriorate significantly after SO_2 pretreatment. It's worth noticing that the diffraction peak at 2θ = 26° becomes much higher after SO_2 treatment. Although it is quite difficult to give precise attribution of this single peak, a reasonable assumption could be that this peak indicate the formation of Titanium sulfate (JCPDS # 18-1406) or Aluminum Titanium sulfate (JCPDS # 28-0035).

3.4 Redox Properties by H_2-TPR

The redox properties of the prepared Ti/Cu-SSZ-13 catalysts were examined by H_2-TPR analyses (Fig. 6). Four major reduction peaks can be observed over all the samples. Based on our previous reports [20, 24] and other reports [25, 34, 35], three peaks (α, β, γ) at temperatures below 500 °C reflect the reduction of different isolated Cu^{2+} species coordinated in various sites of the CHA structure. To be specific, peak α at 181 °C is attributed to the reduction

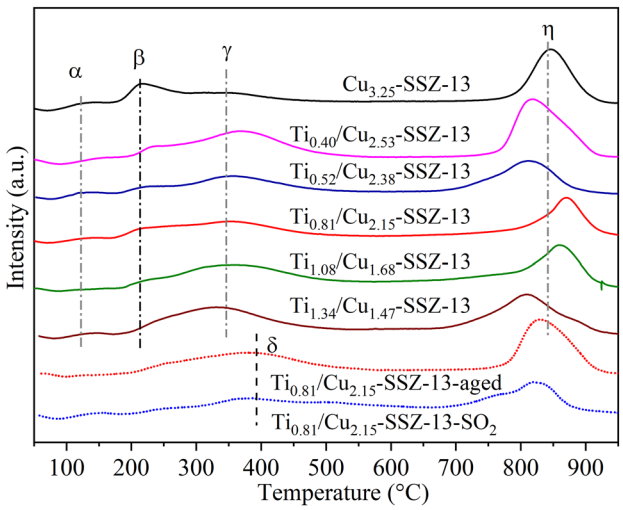

Fig. 6 H_2-TPR profiles of the prepared Ti/Cu-SSZ-13 catalysts

of isolated Cu^{2+} near octagonal window (Cu1 species in site IV); peak β at 249 °C is ascribed to the reduction of isolated Cu^{2+} inside the super cage diverging from the dual hexatomic ring (Cu2 species in Site I); peak γ at 366 °C is assigned to the reduction of isolated Cu^{2+} located in the hexagonal prism center (Cu3 species in Site III). The high temperature peak η above 700 °C corresponds to the reduction of monovalent Cu^{+} to metallic Cu^{0}. No reduction peak assigning to Ti species is observed since titanium oxides are generally reported to be reduced at temperatures higher than 1000 °C. With increasing Ti content, areas of both peak α and peak β diminishes moderately while peak γ is expanded with enlarged area. Various reports [34, 36, 37] have clarified that Cu3 species located at site III are more stable due to greater steric hindrance of the hexagonal prism. Therefore, the peak diminishment with increasing Ti content indicates that Cu1 and Cu2 species gradually disappear due to site occupation by Ti species or possible migration of Cu species, which then leads to unsatisfying low temperature SCR activity of Ti/Cu-SSZ-13 with high Ti contents.

H_2-TPR profiles of $Ti_{0.81}/Cu_{2.15}$-SSZ-13 catalysts after hydrothermal ageing and SO_2 pretreatment are also shown in Fig. 6. Comparing to the fresh catalyst, both peaks α and peak β disappear substantially in the H_2-TPR profile of $Ti_{0.81}/Cu_{2.15}$-SSZ-13-aged sample, indicating significant loss of isolated Cu^{2+} species. Meanwhile, a new peak δ around 460 °C overlapping peak γ appears, which is related to the reduction of small CuO_x agglomerates [38]. These agglomerated CuO_x clusters are most likely to form in the course of hydrothermal ageing period and are considered responsible for facilitating unfavorable NH_3 oxidation [39], thus causing narrower operation temperature windows. Similar TPR profile can be seen for $Ti_{0.81}/Cu_{2.15}$-SSZ-13-SO_2 sample as all three peaks (α, β and γ) diminish and shift to higher temperatures, accompanied by the appearance of peak δ with much smaller area than that of $Ti_{0.81}/Cu_{2.15}$-SSZ-13-aged. These results demonstrate that the relative content of isolated Cu^{2+} species also declined after SO_2 pretreatment, but the formation of CuO_x species was not as severe as that after hydrothermal ageing. Therefore, the high temperature SCR activity of $Ti_{0.81}/Cu_{2.15}$-SSZ-13-SO_2 is relatively better than that of $Ti_{0.81}/Cu_{2.15}$-SSZ-13-aged.

3.5 Surface Chemistry by XPS

The surface chemistry of the prepared Ti/Cu-SSZ-13 catalysts was characterized by XPS analyses. Figure 7 shows the XPS spectra processed via multi-peak fitting method and Table 1 summaries the corresponding element

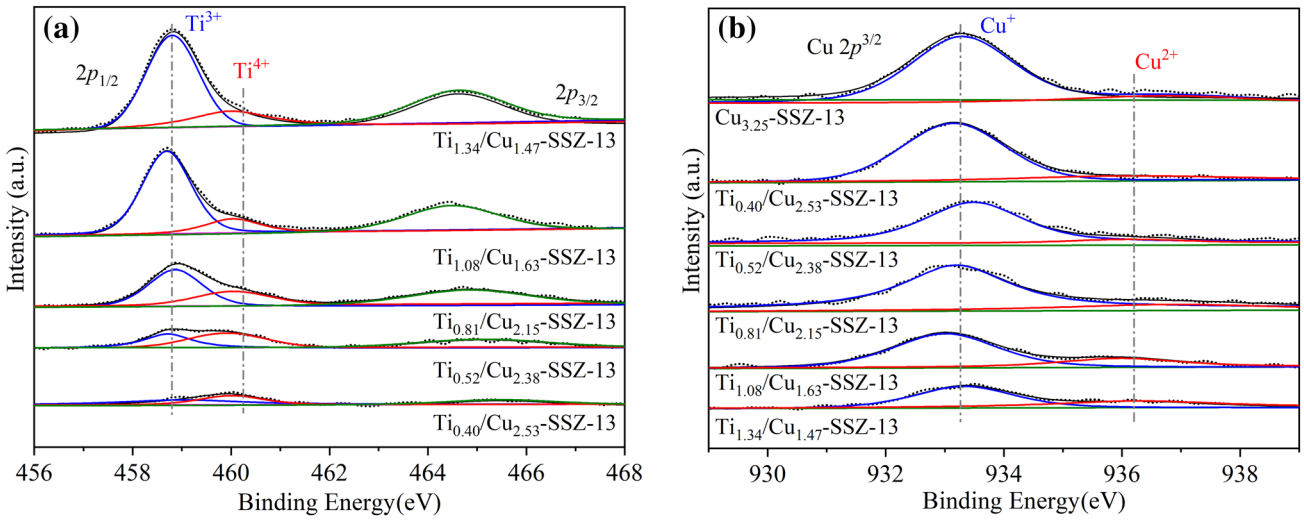

Fig. 7 **a** Ti 2p and **b** Cu 2p XPS spectra of the prepared Ti/Cu-SSZ-13 catalysts

Table 1 Surface element distribution of the prepared Ti/Cu-SSZ-13 catalysts

Samples	Ti^{3+} (at. %)	Ti^{4+} (at. %)	Cu^{+} (at. %)	Cu^{2+} (at. %)
$Cu_{3.25}$-SSZ-13	–	–	2.0	0.21
$Ti_{0.40}/Cu_{2.53}$-SSZ-13	0.04	0.09	1.3	0.20
$Ti_{0.52}/Cu_{2.38}$-SSZ-13	0.19	0.22	1.2	0.17
$Ti_{0.81}/Cu_{2.15}$-SSZ-13	0.52	0.25	1.1	0.16
$Ti_{1.08}/Cu_{1.63}$-SSZ-13	0.62	0.23	0.95	0.13
$Ti_{1.34}/Cu_{1.47}$-SSZ-13	0.83	0.20	0.81	0.08

distribution data. Figure 7a presents the Ti 2p spectra. Two sets of characteristic peaks around 458.0 eV (Ti $2p_{1/2}$) and 464.5 eV (Ti $2p_{3/2}$) can be observed, which can be further differentiated and attributed to Ti^{4+} sepcies (458.5 and 464.5 eV) and Ti^{3+} sepcies (460.2 and 466.2 eV) resepectively [40]. As shown in Table 1, with increasing Ti content, the amount of Ti^{4+} species on the catalyst surfaces increases first and then decreases, following the order of $Ti_{0.81}/Cu_{2.15}$-SSZ-13 > $Ti_{1.08}/Cu_{1.68}$-SSZ-13 > $Ti_{0.52}/Cu_{2.38}$-SSZ-13 > $Ti_{1.34}/Cu_{1.47}$-SSZ-13 > $Ti_{0.40}/Cu_{2.53}$-SSZ-13, which is in consistent with their order of SCR operation temperature window width. Considering that the low temperature activity of all the Ti/Cu-SSZ-13 catalysts are very close, these results suggest that the abundant surface Ti^{4+} species are conducive for elevating the high temperature SCR reactivity. Figure 7b presents the Cu 2p spectra. All the catalysts present typical Cu $2p_{3/2}$ characteristic peaks around 933.0 eV. The Cu $2p_{3/2}$ peaks can be further deconvoluted into two peaks, whereas peak around 933.2 eV represents the surface Cu^{+} species, while peak around 936.2 eV is attributed to isolated Cu^{2+} species coordinated in the SSZ-13 zeolite frame structure [24, 41, 42] as Ti doping content increases, the total amount of Cu species gradually decreases. Meanwhile, the relative content of isolated Cu^{2+} species coordinated in the zeolite framework also slightly decreases possbily due to the occupation of charge compensation sites by Ti species. Since isoltaed Cu^{2+} species are generally recognized as the predominant active species of Cu zeolite catalyts contributing to SCR reactiviy in low temperature ranges, therefore the over-doping of Ti slightly hinders the low temperature NH_3-SCR activities of Ti/Cu-SSZ-13.

3.6 Identification of Ti Species by UV–Vis

To gain better insights regarding the identification of different Ti species in the synthesized Ti/Cu-SSZ-13 catalysts, UV–Vis analyses were conducted, and the obtained spectra are shown in Fig. 8 below together with the peak deconvolution results. The bands observed around 210 nm are assigned to the charge transfer of $O_{zeolite} \rightarrow Cu^{2+}$. Two bands assigning to Ti species can be seen around 220 nm and 280 nm, respectively. The former is attributed to the charge transfer from the excitation of O 2p valent electron to the empty d orbitals of monomeric Ti^{4+} ions, while the latter represents the charge transfer of Ti = O group in the aggregated TiO_x particles over the SSZ-13 surface [43–45]. Table 2 present the relative content of these two Ti species estimated semi-quantitatively based on peak-deconvoluting results. It is quite clear that the monomeric Ti^{4+} species are predominant at lower Ti loading content; while the amount of monomeric Ti^{4+} species turns to decrease and more aggregated TiO_x appears with increasing Ti content. Such evolution between different Ti species

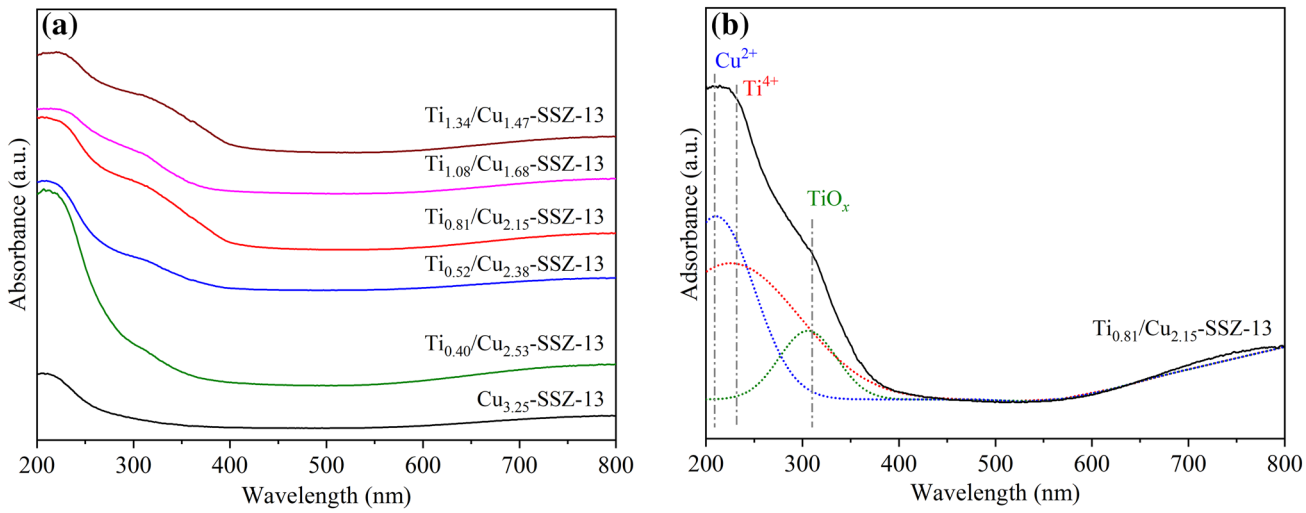

Fig. 8 **a** UV–Vis spectra of the prepared Ti/Cu-SSZ-13 catalysts and **b** peak-deconvoluting of the $Ti_{0.81}/Cu_{2.15}$-SSZ-13 sample

Table 2 Relative content of different Ti species in the prepared Ti/Cu-SSZ-13 catalysts

Samples	Monomeric Ti^{4+} (at. %)	TiO_x (at. %)	Content of monomeric Ti^{4+} (wt. %)
$Ti_{0.40}/Cu_{2.53}$-SSZ-13	82.74	17.26	0.33
$Ti_{0.52}/Cu_{2.38}$-SSZ-13	77.41	22.59	0.40
$Ti_{0.81}/Cu_{2.15}$-SSZ-13	70.15	29.85	0.57
$Ti_{1.08}/Cu_{1.63}$-SSZ-13	50.14	49.86	0.54
$Ti_{1.34}/Cu_{1.47}$-SSZ-13	31.89	68.11	0.43

be elucidated as: at low Ti content, the majority of doped Ti prefers to occupy either protonic charge-compensating H^+ sites or the Si^{4+} sites in the frame structure of SSZ-13 zeolite; Increasing Ti loading leads to saturation of these protonic H^+ sites and the Si^{4+} sites, thus the over doped Ti is very likely to aggregate over catalyst's surface and thereby decreasing the relative content of monomeric Ti^{4+} species. Combining activity evaluation results above, we can see that the distribution and chemical state of different Ti species mainly affect the high temperature NH_3-SCR reactivity of the Ti/Cu-SSZ-13 catalyst. Higher content of mononuclear Ti^{4+} species could improve the high temperature reactivity, while the presence of more aggregated TiO_x would lead to the narrowed operation temperature window instead. $Ti_{0.81}/Cu_{2.15}$-SSZ-13 sample synthesized via in situ one-pot strategies not only contains more mononuclear Ti^{4+} species, but also has relatively low content of surface aggregated TiO_x specie, therefore presents the best NH_3-SCR catalytic performances.

3.7 Discussions of the Correlations Between Active Species and SCR Reactivity

Various previous studies have focused on the identification of active Cu species for the NH_3-SCR over Cu-SSZ-13 zeolites. Series of different forms of Cu species such as isolated Cu^{2+}/Cu^+ species, dimeric Cu species as well as CuO_x have all been suggested to be active sites. Wang et al. [14, 46] demonstrated that for Cu-based small-pore zeolites, agglomerated CuO_x clusters are very unlike to be the primary active sites as CuO_x clusters would accelerate the unfavorable NH_3 oxidation. Giordanino et al. [47] reported that dimeric Cu species contribute very little to SCR reactivity as they are quite unlikely to exist stably in Cu-SSZ-13. Bates et al. [48] suggested that the kinetically rate-determining steps for standard SCR mainly take place on the isolated Cu^{2+} species located in exchange sites via UV–Vis-NIR and XAS identifications. Zhang et al. [26] reported that the isolated Cu^{2+} ions play significant roles in maintaining higher NH_3-SCR activity at low-temperature in Fe-Cu-SSZ-13 catalyst using UV–Vis and EPR analyses. Our previous research

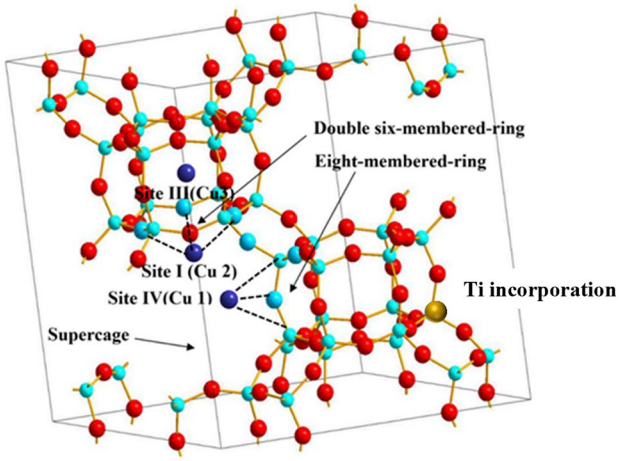

Fig. 9 Simplified schematic illustration of the $Ti_{0.81}/Cu_{2.15}$-SSZ-13 catalyst

[20] demonstrated that for Cu-SSZ-13 isolated Cu^{2+} species exist in three different forms, which are contributive for low-temperature NH_3-SCR activity improvement. In the current work, neither dimeric Cu species nor CuO_x clusters are observed, but instead isolated Cu^{2+} species along with Cu^+ are evidenced as the primary existing Cu species. Considering the reduction temperature of Cu^+ goes high above 700 °C, Cu^+ species can be reasonably ruled out to be possible active sites. Hence, we hereby propose that excellent low temperature reactivity of Ti/Cu-SSZ-13 relies on to the contribution of isolated Cu^{2+} species (Fig. 9). With increasing Ti doping content, these isolated Cu^{2+} species partially decreases possbily due to sites occupation by Ti, thus the low temperature SCR reactivity is slightly deterred.

On the other hand, effective improvement of NH_3-SCR activity at high temperatures by doping transitional metal ions into Cu-SSZ-13 system have also been confirmed by many studies. Our previous studies [24] demonstrated that doping Fe into Cu-SSZ-13 could generate sufficient monomeric Fe^{3+} species, acting as critical sites for sustaining the high temperature SCR activity, which are in good consistent with other researchers' reports [21–23]. However, the strong oxidizing ability of multi valent transitional metal ions (for example Fe^{3+}) would facilitate undesired NH_3 oxidation [49]. Hence, Ti with moderate oxidation ability and with weak acidity could be proper substitution. On one hand, Gu et al. [50] and Geng et al. [51] reported that the introduction of Ti species can improve the surface acidity, which is beneficial for the adsorption of NH_3, and finally enhances the SCR performance. Song et al. [52] revealed that Ti doping can also lower the activation energy for NO oxidation step via DFT calculations. In the present work, the monomeric Ti^{4+} species are verified as predominant Ti species. According to the above literatures and combing the

activity-structure results, it can be proposed that the dominant active sites for low temperature SCR reaction can be ascribed to isolated Cu^{2+} species, while high temperature SCR reactivity mainly relies on the contribution of monomeric Ti^{4+} species, therefore by introducing proper amount of Ti into Cu-SSZ-13 can significantly expand its operation temperature windows width. On the other hand, Kunitake et al. [53] proposed that incorporation of a small amount of Ti into the CHA framework may have decreased the stress of the zeolite framework, thus being very useful to improve the thermal/hydrothermal stability. Imasaka [54] revealed that crystal structure of the zeolites collapsed because of the desorption of Al from the framework after ageing while improvement of the thermal stability over Ti-CHA zeolite was expected owing to the he incorporation of Ti and substitution of aluminum into the zeolite framework. Therefore, Ti introduced Cu/Ti-SSZ-13 also exhibited high hydrothermal stability. However, Ti over doping would result in partial destruction of the zeolite structure, occupation of Cu^{2+} cation sites and formation of surface aggregated TiO_x species, thus leading to unsatisfactory NH_3-SCR performances.

Moreover, although the affection of hydrothermal ageing and SO_2 poisoning on active species evolution requires further in-depth studies and was not deeply discussed in the current manuscript, a brief explanation is proposed as follows. For Cu species, the above H_2-TPR results suggest agglomerated CuO_x species formed during hydrothermal ageing possibly due to migration of isolated Cu^{2+} species. While after SO_2 pretreatment, our previous EPR studies [20] on SO_2 pretreated Cu-SSZ-13 samples shows that the coordination environment of Cu^{2+} species didn't change a lot and the content of isolated Cu^{2+} species decreased due to blockage by sulfate species formed during SO_2 pretreatment, which are considered responsible for activity deterioration in the tolerability tests. For Ti species, since most of the featured CHA structure can be preserved in a certain degree during hydrothermal ageing, thus it's reasonable to deduce that most of Ti could still be incorporated into zeolite framework after hydrothermal ageing. While after SO_2 pretreatment, both the XRD and *ex-situ* FITR (see the supplymentary information) results indicate the existence of surface sulfates, thereby deteriorating NH_3-SCR activity.

4 Conclusion

Ti/Cu-SSZ-13 zeolite catalysts with variable Ti loading content were prepared via convenient *in-situ* one-pot synthesizing strategy and underwent systematic NH_3-SCR performance evaluations. Among the Ti/Cu-SSZ-13 catalysts tested, the optimized $Ti_{0.81}/Cu_{2.15}$-SSZ-13 catalyst in this work presents wide-expanded operation temperature window width ranging from 140 to 540 °C, excellent N_2 selectivity along with superior H_2O/SO_2 tolerability, making it potential candidate for diesel-engines exhaust purification. Detailed characterizations demonstrate that the synthesized Ti/Cu-SSZ-13 catalysts present well-crystallized characteristic CHA structure. The catalytic advantages of $Ti_{0.81}/Cu_{2.15}$-SSZ-13 catalyst can be ascribed to the contribution of both Cu and Ti active species, as the isolated Cu^{2+} species serve as major active sites for SCR reaction at low temperatures, while the abundant monomeric Ti^{4+} species are conducive for improving the high temperature SCR activity. Ti over doping contrarily leads to inferior NH_3-SCR reactivity, resulting from partially- destructed zeolite structure, occupation of Cu^{2+} cation sites as well as formation of surface aggregated TiO_x species. Besides, hydrothermal ageing causes formation of agglomerated CuO_x while sulfate species generated during SO_2 pretreatment block surface active sites, therefore explaining the corresponding activity deterioration.

Supplementary Information The online version contains supplementary material available at https://doi.org/10.1007/s10563-022-09374-8.

Acknowledgements This work was financially supported by the Key Program of Science Technology Department of Zhejiang Province (No.2018C03037), the Natural Science Foundation of the Jiangsu Higher Education Institutions of China (20KJB610005), the Natural Science Foundation of Jiangsu Province (BK20201037, BK20190705), Key Research and Development Program of Anhui Province (202104g01020006) and the Scientific Research Fund of Nanjing Institute of Technology (No. YKJ2019111 and No. YKJ2019110).

Author Contribution All authors have contributed the creation of this manuscript. JW: Conceptualization, Methodology, Validation, Investigation, Data curation, Visualization, Writing—original draft, Funding acquisition. JC: Methodology, Validation, Investigation, Data curation, Visualization. YS: Investigation, Validation, Data curation. YW: Methodology, Validation, Investigation, Data curation. YL: Investigation, Funding acquisition, Writing—review & editing. JZ: Investigation, Funding acquisition, Writing—review & editing. GW: Resources, Investigation, Funding acquisition. RZ: Conceptualization, Resources, Funding acquisition, Project administration, Supervision, Writing—review & editing.

Declarations

Conflict of interest On behalf of all authors, the corresponding author states that there is no conflict of interest.

References

1. Boretti A (2017) The future of the internal combustion engine after "diesel-gate." SAE Technical Paper, p 1933
2. Joshi A (2019) Review of vehicle engine efficiency and emissions. SAE Int J Adv Curr Prac Mobility 1:734–761
3. Pourvakhshoori N, Khankeh HR, Stueck M, Farrokhi M (2020) The association between air pollution and cancers: controversial evidence of a systematic review. Environ Sci Pollut Res 27:38491–38500

4. Qu Y, An J, He Y, Zheng J (2016) An overview of emissions of SO_2 and NO_x and the long-range transport of oxidized sulfur and nitrogen pollutants in East Asia. J Environ Sci 44:13–25
5. Shelef M, McCabe RW (2000) Twenty-five years after introduction of automotive catalysts: what next? Catal Today 62:35–50
6. Zhang NQ, He H, Wang DS, Li YD (2020) Challenges and opportunities for manganese oxides in low-temperature selective catalytic reduction of NO_x with NH_3: H_2O resistance ability. J Solid State Chem 289:121464
7. Lian ZH, Li YJ, Shan WP, He H (2020) Recent progress on improving low-temperature activity of vanadia-based catalysts for the selective catalytic reduction of NOx with ammonia. Catalysts 10:1421
8. Topsøe NY (1994) Mechanism of the selective catalytic reduction of nitric oxide by ammonia elucidated by in situ on-line Fourier transform infrared spectroscopy. Science 265:1217–1219
9. Liu JN, Huang Y, Li HY, Duan HR (2022) Recent advances in removal techniques of vanadium from water: a comprehensive review. Chemosphere 287:132021
10. Szymaszek A, Samojeden B, Motak M (2020) The deactivation of industrial SCR catalysts—a short review. Energies 13:3870
11. Zhang QJ, Wu YF, Yuan HR (2020) Recycling strategies of spent V_2O_5-WO_3/TiO_2 catalyst: a review. Resour Conserv Recy 161:104983
12. Ma YY, Liu Y, Li ZF, Geng C, Bai XF, Cao DX (2020) Synthesis of CuCe co-modified mesoporous ZSM-5 zeolite for the selective catalytic reduction of NO by NH_3. Environ Sci Pollut Res 27:9935–9942
13. Mohan S, Dinesha P, Kumar S (2020) NO_x reduction behaviour in copper zeolite catalysts for ammonia SCR systems: a review. Chem Eng J 384:123253
14. Wang L, Gaudet JR, Li W, Weng D (2013) Migration of Cu species in Cu/SAPO-34 during hydrothermal ageing. J Catal 306:68–77
15. Andana T, Rappe KG, Gao F, Szanyi J, Pereira-Hernandez X, Wang Y (2021) Recent advances in hybrid metal oxide–zeolite catalysts for low-temperature selective catalytic reduction of NO_x by ammonia. Appl Catal B Environ 291:120054
16. Liu ZQ, Jiang H, Guan B, Wei YF, Wu XZ, Lin H, Huang Z (2022) Optimizing the distribution and proportion of various active sites for better NH3-SCR property over Cu/SSZ-13. Environ Sci Pollut Res 29:19447–19459
17. Shan YL, Du JP, Zhang Y, Shan WP, Shi XY, Yu YB, Zhang RD, Meng XJ, Xiao FS, He H (2021) Selective catalytic reduction of NO_x with NH_3: opportunities and challenges of Cu-based small-pore zeolites. Natl Sci Rev 8:nwabo10
18. Gao F, Mei DH, Wang YL, Szanyi J, Peden CHF (2017) Selective catalytic reduction over Cu/SSZ-13: linking homo- and heterogeneous catalysis. J Am Chem Soc 139:4935–4942
19. Kwak JH, Tonkyn RG, Kim DH, Szanyi J, Peden CHF (2010) Excellent activity and selectivity of Cu-SSZ-13 in the selective catalytic reduction of NO_x with NH_3. J Catal 275:187–190
20. Chen JW, Zhao R, Zhou RX (2018) A new insight into active Cu^{2+} species properties in one-pot synthesized Cu-SSZ-13 catalysts for NO_x reduction by NH_3. ChemCatChem 10:5182–5189
21. Yin CY, Cheng PF, Li X, Yang RT (2016) Selective catalytic reduction of nitric oxide with ammonia over high-activity Fe/SSZ-13 and Fe/one-pot-synthesized Cu-SSZ-13. Catal Sci Technol 6:7561–7568
22. Wang JC, Peng ZL, Qiao H, Yu HF, Hu YF, Chang LP, Bao WR (2016) Cerium-stabilized Cu-SSZ-13 catalyst for the catalytic removal of NO_x by NH_3. In Eng Chem Res 55:1174–1182
23. Zhao ZC, Yu R, Shi C, Gies H, Xiao FS, De Vos D, Yokoi T, Bao XH, Kolb U, McGuire R, Parvulescu AN, Maurer S, Müller U, Zhang WP (2019) Rare-earth ion exchanged Cu-SSZ-13 zeolite from organotemplate-free synthesis with enhanced hydrothermal stability in NH_3-SCR of NO_x. Catal Sci Technol 9:241–251
24. Wan J, Chen JW, Zhao R, Zhou RX (2021) One-pot synthesis of Fe/Cu-SSZ-13 catalyst and its highly efficient performance for the selective catalytic reduction of nitrogen oxide with ammonia. J Environ Sci 100:306–316
25. Zhang RR, Li YH, Zhen TL (2014) Ammonia selective catalytic reduction of NO over Fe/Cu-SSZ-13. RSC Adv 4:52130–52139
26. Zhang T, Li JM, Liu J, Wang DX, Zhao Z, Cheng K, Li JH (2015) High activity and wide temperature window of Fe-Cu-SSZ-13 in the selective catalytic reduction of NO with ammonia. AIChE J 61:3825–3837
27. Hammershøi PS, Jangjou Y, Epling WS, Jensen AD, Janssens TVW (2018) Reversible and irreversible deactivation of Cu-CHA NH_3-SCRcatalysts by SO_2 and SO_3. Appl Catal B Environ 226:38–45
28. Shan YL, Shi XX, Yan ZD, Liu JJ, Yu YB, He H (2019) Deactivation of Cu-SSZ-13 in the presence of SO_2 during hydrothermal ageing. Catal Today 320:84–90
29. Wang AY, Wang YL, Walter ED, Washton NM, Guo YL, Lu GZ, Peden CHF, Gao F (2019) NH_3-SCR on Cu, Fe and Cu+ Fe exchanged beta and SSZ-13 catalysts: Hydrothermal ageing and propylene poisoning effects. Catal Today 320:91–99
30. Zones SI, Van Nordstrand RA (1988) Novel zeolite transformations: the template mediated conversion of cubic-P zeolite to SSZ-13. Zeolites 8:166–174
31. Di Iorio JR, Gounder R (2016) Controlling the isolation and pairing of aluminum in chabazite zeolites using mixtures of organic and inorganic structure-directing agents. Chem Mater 28:2236–2247
32. Deka U, Juhin A, Eilertsen EA, Emerich H, Green MA, Korhonen ST, Weckhuysen BM, Beale AM (2012) Confirmation of isolated Cu^{2+} ions in SSZ-13 zeolite as active sites in NH_3-selective catalytic reduction. J Phys Chem C 116:4809–4818
33. Mrak M, Tušar NN, Logar NZ, Mali G, Kljajić A, Arčon I, Launay F, Gedeon A, Kaučič V (2006) Titanium containing microporous/mesoporous composite (Ti, Al)-Beta/MCM-41: synthesis and characterization. Micropor Mesopor Mat 95:76–85
34. Gao F, Walter ED, Karp EM, Luo JY, Tonkyn RG, Kwak JH, Szanyi J, Peden CHF (2013) Structure–activity relationships in NH3-SCR over Cu-SSZ-13 as probed by reaction kinetics and EPR studies. J Catal 300:20–29
35. Kwak JH, Zhu HY, Lee JH, Peden CHF, Szanyi J (2012) Two different cationic positions in Cu-SSZ-13? Chem Commun 48:4758–4760
36. Chen ZQ, Guo L, Qu HX, Liu L, Xie HF, Zhong Q (2020) Controllable positions of Cu^{2+} to enhance low-temperature SCR activity on novel Cu-Ce-La-SSZ-13 by a simple one-pot method. Chem Commun 56:2360–2363
37. Xie LJ, Liu FD, Ren LM, Shi XY, Xiao FS, He H (2014) Excellent performance of one-pot synthesized Cu-SSZ-13 catalyst for the selective catalytic reduction of NO_x with NH_3. Environ Sci Technol 48:566–572
38. Kim YJ, Lee JK, Min KM, Hong SB, Nam IS, Cho BK (2014) Hydrothermal stability of CuSSZ13 for reducing NO_x by NH_3. J Catal 311:447–457
39. Han J, Wang AY, Isapour G, Härelind H, Skoglundh M, Creaser D, Olsson L (2021) N_2O formation during NH_3-SCR over different zeolite frameworks: effect of framework structure, copper species, and water. Ind Eng Chem Res 60:17826–17839
40. Shi YJ, Guo XL, Wang YY, Kong FZ, Zhou RX (2022) New insight into the design of highly dispersed Pt supported CeO2-TiO2 catalysts with superior activity for VOCs low-temperature removal. Green Energy Environ online. https://doi.org/10.1016/j.gee.2022.03.009

41. Han S, Cheng J, Zheng CK, Ye Q, Cheng SY, Kang TF, Dai HX (2017) Effect of Si/Al ratio on catalytic performance of hydrothermally aged Cu-SSZ-13 for the NH_3-SCR of NO in simulated diesel exhaust. Appl Surf Sci 419:382–392
42. Yu R, Zhao ZC, Huang SJ, Zhang WP (2020) Cu-SSZ-13 zeolite–metal oxide hybrid catalysts with enhanced SO_2-tolerance in the NH_3-SCR of NO_x. Appl Catal B Environ 269:118825
43. Bourezgui A, Kacem I, Daoudi M, Al-Hossainy AF (2020) Influence of gamma-irradiation on structural, optical and photocatalytic performance of TiO_2 nanoparticles under controlled atmospheres. J Electron Mater 49:1904–1921
44. Thangaraj A, Kumer R, Mirajkar SP, Ratnasamy P (1991) Catalytic properties of crystalline titanium silicalites I. Synthesis and characterization of titanium-rich zeolites with MFI structure. J Catal 130:1–8
45. Zhou DH, Zhang HJ, Zhang JJ, Sun XM, Li HC, He N, Zhang WP (2014) Density functional theory investigations into the structure and spectroscopic properties of the Ti^{4+} species in Ti-MWW zeolite. Micropor Mesopor Mat 195:216–226
46. Wang L, Li W, Qi GS, Weng D (2012) Location and nature of Cu species in Cu/SAPO-34 for selective catalytic reduction of NO with NH_3. J Catal 289:21–29
47. Giordanino F, Vennestrøm PNR, Lundegaard LF, Stappen FN, Mossin S, Beato P, Bordigaa S, Lamberti C (2013) Characterization of Cu-exchanged SSZ-13: a comparative FT-IR, UV-Vis, and EPR study with Cu-ZSM-5 and Cu-β with similar Si/Al and Cu/Al ratios. Dalton Trans 42:12741–12761
48. Bates SA, Verma AA, Paolucci C, Parekh AA, Anggara T, Yezerets A, Schneider WF, Miller JT, Delgass WN, Ribeiro FH (2014) Identification of the active Cu site in standard selective catalytic reduction with ammonia on Cu-SSZ-13. J Catal 312:87–97
49. Ellmers I, Vélez RP, Bentrup U, Brückner A, Grünert W (2014) Oxidation and selective reduction of NO over Fe-ZSM-5–How related are these reactions? J Catal 311:199–211
50. Gu JL, Duan RD, Chen WB, Chen Y, Liu LL, Wang XD (2020) Promoting effect of Ti species in MnO_x-FeO_x/silicalite-1 for the low-temperature NH_3-SCR reaction. Catalysts 10:566
51. Geng Y, Chen XL, Yang SJ, Liu FD, Shan WP (2017) Promotional effects of Ti on a CeO_2–MoO_3 catalyst for the selective catalytic reduction of NO_x with NH_3. ACS Appl Mate Inter 9:16951–16958
52. Song ZJ, Wang B, Yu J, Ma C, Chen T, Yang W, Liu S, Sun LS (2018) Effect of Ti doping on heterogeneous oxidation of NO over Fe_3O_4 (1 1 1) surface by H_2O_2: a density functional study. Chem Eng J 354:517–524
53. Kunitake Y, Takata T, Yamasaki Y, Yamanaka N, Tsunoji N, Takamitsu Y, Sadakane M, Sano T (2015) Synthesis of titanated chabazite with enhanced thermal stability by hydrothermal conversion of titanated faujasite. Micropor and Mesopor Mat 215:58–66
54. Imasaka S, Ishii H, Hayashi JI, Araki S, Yamamoto H (2019) Synthesis of CHA-type titanosilicate zeolites using titanium oxide as Ti source and evaluation of their physicochemical properties. Micropor and Mesopor Mat 273:243–248